

# Surface Properties and Platelet Adhesion Characteristics of Acrylic Acid and Allylamine Plasma-Treated Polyethylene

TZE-MAN KO and STUART L. COOPER\*

University of Wisconsin, Department of Chemical Engineering, Madison, Wisconsin 53706

## SYNOPSIS

Acidic oxygen-containing and basic nitrogen-containing functional groups were incorporated onto thin films formed by plasma polymerization of acrylic acid and allylamine in a low-pressure glow discharge. ESCA, ATR-FTIR spectroscopy, and static contact-angle measurements confirmed the presence of these functional groups. Surface hydrophilicity of the acrylic acid plasma polymer decreased with time due to the diffusion of hydrophilic oxygen-containing functional groups away from the surface of the plasma-treated polyethylene. In contrast, the hydrophilicity of the allylamine plasma polymer increased with time because of the extensive post-plasma-treatment oxidation with atmospheric oxygen. In assessing the blood compatibility of these two types of plasma polymer surfaces by platelet adhesion and spreading, the acidic acrylic acid plasma polymers showed an improvement in thromboresistance, but the basic allylamine plasma polymers were more thrombogenic than was the untreated low-density polyethylene base material. © 1993 John Wiley & Sons, Inc.

## INTRODUCTION

Plasma polymerization is the formation of polymeric materials typically in a low-pressure glow discharge. The materials formed by plasma polymerization are vastly different from conventional polymers and constitute a new kind of insoluble, infusible, and highly cross-linked polymer. Yasuda suggested that plasma polymerization is an "atomic" process as compared to the traditional "molecular" polymerization process.<sup>1</sup>

Recently, plasma polymerization has been applied to prepare novel polymeric biomaterials.<sup>1-5</sup> The capability of plasmas to alter surface physical and chemical properties without affecting the bulk properties of the base material is advantageous in the design, development, and manufacturing of biocompatible polymers. It is important to determine the effects of different functional groups on a material's surface, physical, chemical, and blood-contacting properties for the application of certain biomaterials. In this work, acrylic acid and allylamine were plasma-polymerized to create thin films of acidic and basic surface properties on low-density polyethylene. It is expected that oxygen- and nitro-

gen-containing species can be generated from acrylic acid and allylamine plasmas, respectively. As a result, some degree of hydrophilic carboxylic or amino functionality can be incorporated by plasma polymerization of these two monomers.<sup>6-12</sup>

Low-density polyethylene (LDPE) is a commonly used biomaterial that possesses fairly good grafting reactivity compared to other common polymeric materials. A number of plasma modification and plasma polymerization systems have been employed in order to introduce oxygen-containing functional groups onto polyethylene surfaces for biomaterial applications.<sup>13-15</sup> The aim of this work was to determine some of the plasma polymerization parameters for the acrylic acid and allylamine plasma reactions and to characterize these two types of plasma polymer thin films by ESCA, ATR-FTIR spectroscopy, contact-angle measurements, profilometry, and SEM. Platelet adhesion and activation studies were used to assess the blood compatibility of these two plasma polymers.

## PLASMA REACTOR

A 1 in. OD quartz tubular plasma reactor was externally capacitively-coupled by two copper electrodes (Fig. 1). The energy for the plasma reaction

\* To whom correspondence should be addressed.

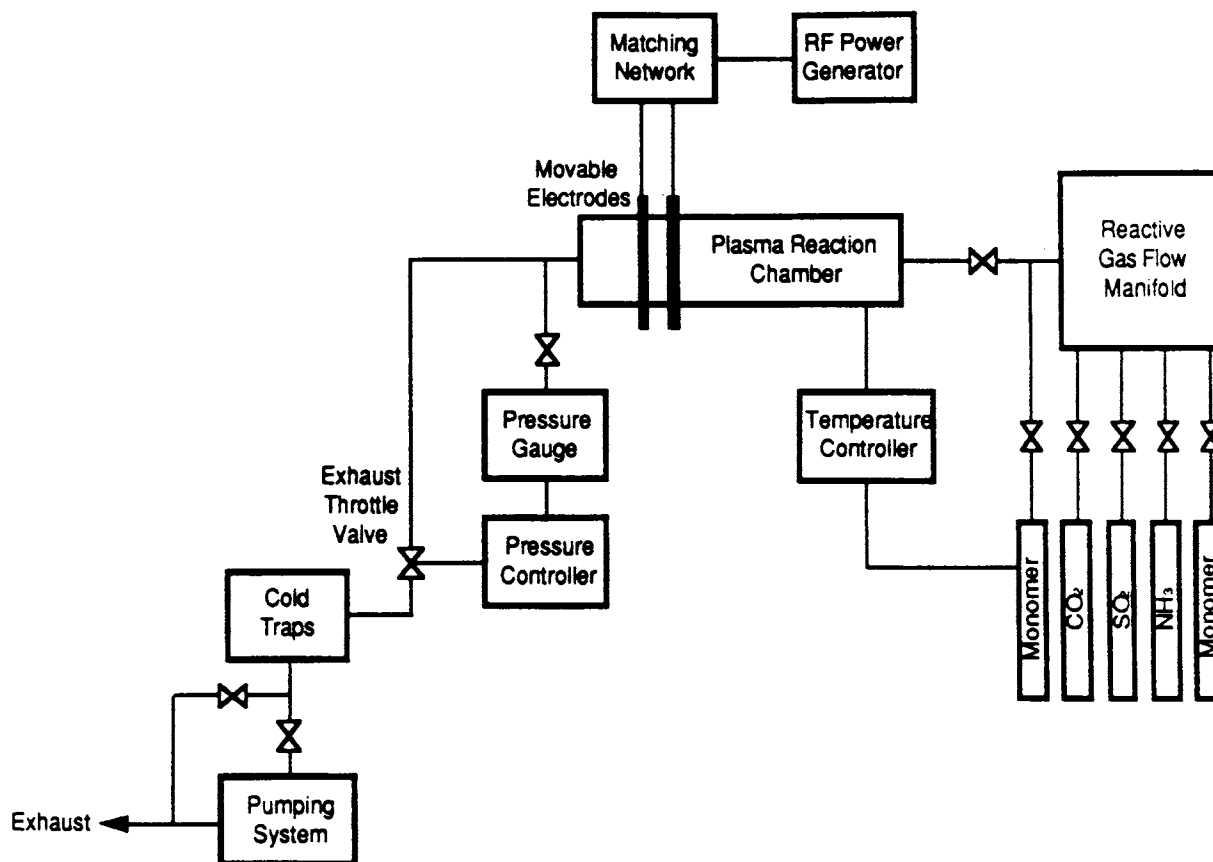


Figure 1 Schematic representation of the plasma polymerization reactor system.

was supplied by a 13.56 MHz rf ENI ACG-3 plasma generator. An automatic ENI TH-1000 matching network was connected in series between the power generator and the external copper electrodes for maximum power transfer. The gas flow rates of the reactive gases and monomers were monitored by MKS MASS-FLO™ 1160B mass flow controllers. An SSL portable temperature controller was used to vaporize the liquid monomers. The plasma reactor system was pumped down by a Leybold TRIVAC D30A rotary vane pump. The pressure of the system was regulated by an MKS 253A exhaust throttle valve and a 252C exhaust throttle valve controller. Pressure readings were made using an MKS 127A Baratron absolute pressure transducer.

## MATERIALS AND METHODS

### Plasma Treatment

Rectangular samples, 0.75 × 1.00 in., were cut from LDPE roll film (Penn Fibre). A sample was then

placed 15 in. from the inlet inside a 2 ft × 1 in. OD quartz tubular plasma reactor. Two external copper electrodes separated by 3.5 in. were located across the rectangular sample. The base pressure of the system was then pumped down to below 1 mTorr. Acrylic acid [CH<sub>2</sub>=CHC(O)OH] is a liquid monomer; therefore, additional vaporization procedures were needed to feed it into the plasma reactor. By the use of heating tapes and temperature controllers, the monomer and the plasma reactor were kept at a constant temperature of 60°C during the experiment. The flow of acrylic acid was monitored by a metering valve so that its vapor pressure inside the plasma reactor chamber was 10 mTorr above the base pressure of the system. After the system pressure was stabilized with a continuous flow of the reactive gas, it was regulated to 200 mTorr by the exhaust throttle valve controller. The plasma was ignited for 10 min. Afterward, the plasma power was turned off, the metering valve was closed, the exhaust valve was opened, and the plasma reactor was vented to atmosphere. The plasma-treated sample was then taken out for analysis. Plasma po-

lymerization of acrylic acid was carried out at plasma energy levels of 10, 30, and 50 W. Transparent highly cross-linked thin films were formed on the LDPE substrates by the plasma polymerization of acrylic acid.

Allylamine ( $\text{CH}_2=\text{CHCH}_2\text{NH}_2$ ) is a fairly volatile monomer liquid and it was siphoned into the plasma reactor by vacuum without heating. It was vaporized at a pressure of 10 mTorr above the base pressure of the system. When the system pressure was stabilized with a continuous flow of the monomer, it was then regulated to 200 mTorr by the exhaust throttle valve controller. Plasma polymerization of allylamine was carried out at 5, 10, 30, and 50 W for 10 min. Brownish yellow films were formed on the LDPE substrates.

### ESCA

The surface elemental compositions of both the acrylic acid and allylamine plasma polymers were analyzed by a Perkin-Elmer PHI 5400 ESCA System with its packaged ESCA software. The X-ray source was generated with a Mg anode energized at 15 kV and 300 W. The distance between the sample surface and the tip of the X-ray source anode was maintained constant at about 1.5 in. The aperture of the spherical capacitor electron energy analyzer was set at a diameter of 4 mm so that the area of the sample surface to be analyzed was about 1.3 mm in diameter. Both ESCA survey and multiplex spectra of the plasma-treated LDPE were collected at takeoff angles ( $\theta$ ) of 10°, 30°, 45°, and 75° with respect to the spherical capacitor electron energy analyzer.<sup>16</sup> Angle-dependent ESCA studies were carried out immediately after plasma polymerization. For investigation of the time dependence of the surface concentrations, the angle-dependent ESCA experiment was performed again 6 and 7 days after the acrylic acid and allylamine plasma polymer deposition, respectively.

### ATR-FTIR

FTIR spectroscopy was performed with an attenuated total reflectance (ATR) plate in order to identify the functional groups formed by the acrylic acid and allylamine plasma polymerization. The ATR plate (or internal reflection element [IRE]) used in this experiment was a  $50 \times 20 \times 3$  mm single-pass parallelepiped germanium single crystal with a 45° aperture angle. It was polished by a Buehler® polishing cloth (Microcloth, cat. no. 40-7206) with deionized water and absolute alcohol as the wetting

and lubricating agents. Then, it was dried in a vacuum oven for at least 1 hour. An FTIR background spectrum was taken of the cleaned IRE to make sure that it was free of adsorbed water vapor ( $\nu = 1310\text{--}2000 \text{ cm}^{-1}$ ) and carbon dioxide ( $\nu = 2220\text{--}2380 \text{ cm}^{-1}$ ).<sup>17</sup> The cleaned and dried IRE was then placed inside the plasma reactor for plasma polymer deposition. A plasma polymer was deposited on both sides of the IRE after 30 min of plasma exposure. An FTIR spectrum was collected again. After subtraction of the FTIR background spectrum, a net FTIR spectrum of the acrylic acid or allylamine plasma polymer was obtained.

### Contact Angle

Static sessile drop contact-angle measurements were carried out in deionized double-distilled water for surface hydrophilicity determination. An air or *n*-octane bubble ( $\approx 2 \mu\text{L}$ ) was placed underneath the plasma-treated LDPE sample surface by a microliter syringe and a photograph was taken. The air or *n*-octane contact angle of the plasma-treated material was computed from this photograph.<sup>18</sup> Both air and octane contact-angle experiments were performed for the acrylic acid and allylamine plasma-treated LDPE at two different periods, i.e., immediately after plasma polymerization and about 1 week later. For contact-angle experiments carried out at about 1 week after the plasma treatment, the samples were kept in small glass vials and left in air at room temperature.

### Profilometry

The deposition rates ( $d$ ) of the acrylic acid and allylamine plasma polymers formed by plasma polymerization were determined by profilometry. Cleaned glass coverslips (Corning Cover Glass) were chosen as the substrates for the plasma polymer thin-film deposition because of their hardness and surface smoothness. Before insertion into the plasma polymerization reaction chamber, half of the glass coverslip surface was covered by another piece of coverslip. As a result, a step would be created on the coverslip between the covered and uncovered surfaces after plasma polymerization. The height of this step was measured with a Tencor Instruments Alpha-Step® 200 profilometer with a stylus force of 20 mg.

### Platelet Adhesion

To determine the blood compatibility of the plasma-treated materials, platelet adhesion studies were

**Table I** ESCA Results for the Acrylic Acid Plasma Polymer Deposited on LDPE

Takeoff Angle (Degrees)	Atomic Concentration (%)							
	Immediately after Plasma Polymerization		6 Days after Plasma Polymerization		Immediately after Plasma Polymerization		6 Days after Plasma Polymerization	
	C	O	C	O	C	O	C	O
	10 W (10 min)				30 W (10 min)			
10	17.73	82.27	23.98	76.02	25.02	74.98	29.29	70.71
30	15.56	84.44	22.40	77.60	19.08	80.92	24.66	75.34
45	12.71	87.29	21.33	78.67	15.27	84.73	22.82	77.18
75	15.46	84.54	19.54	80.46	15.71	84.29	21.83	78.17
	50 W (10 min)							
10	28.75	71.25	31.90	68.10				
30	25.76	74.24	26.92	73.08				
45	19.97	80.03	24.07	75.93				
75	21.23	78.77	23.68	76.32				

conducted since platelet adhesion is one of the most important steps during blood coagulation on artificial surfaces.<sup>19-21</sup> Blood samples were drawn from

healthy canines (adult mongrel dogs) that were not on medication. Platelet-rich plasma was obtained and the platelets were washed by albumin density

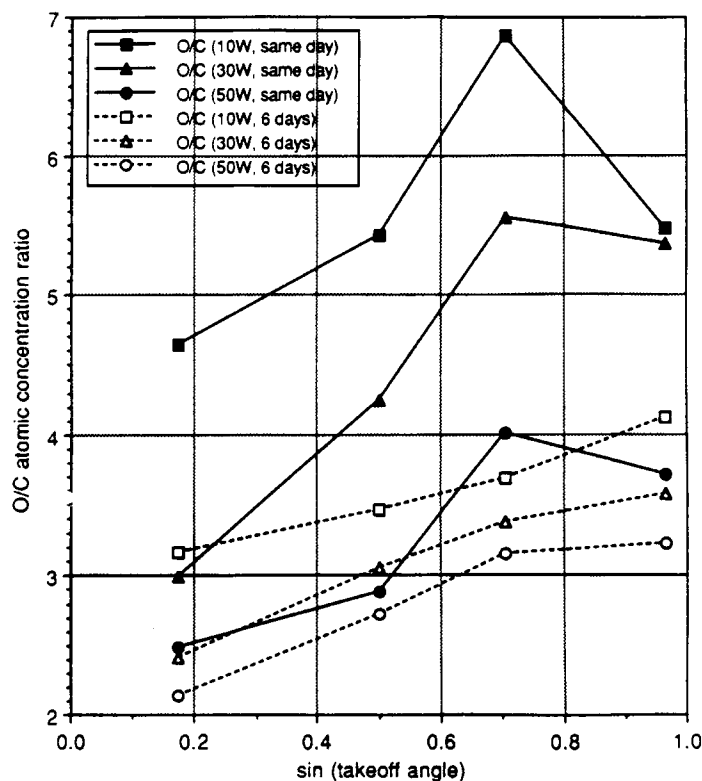


**Figure 2** O/C atomic concentration ratio vs.  $\sin \theta$  for the acrylic acid plasma polymer deposited on LDPE (10 min).

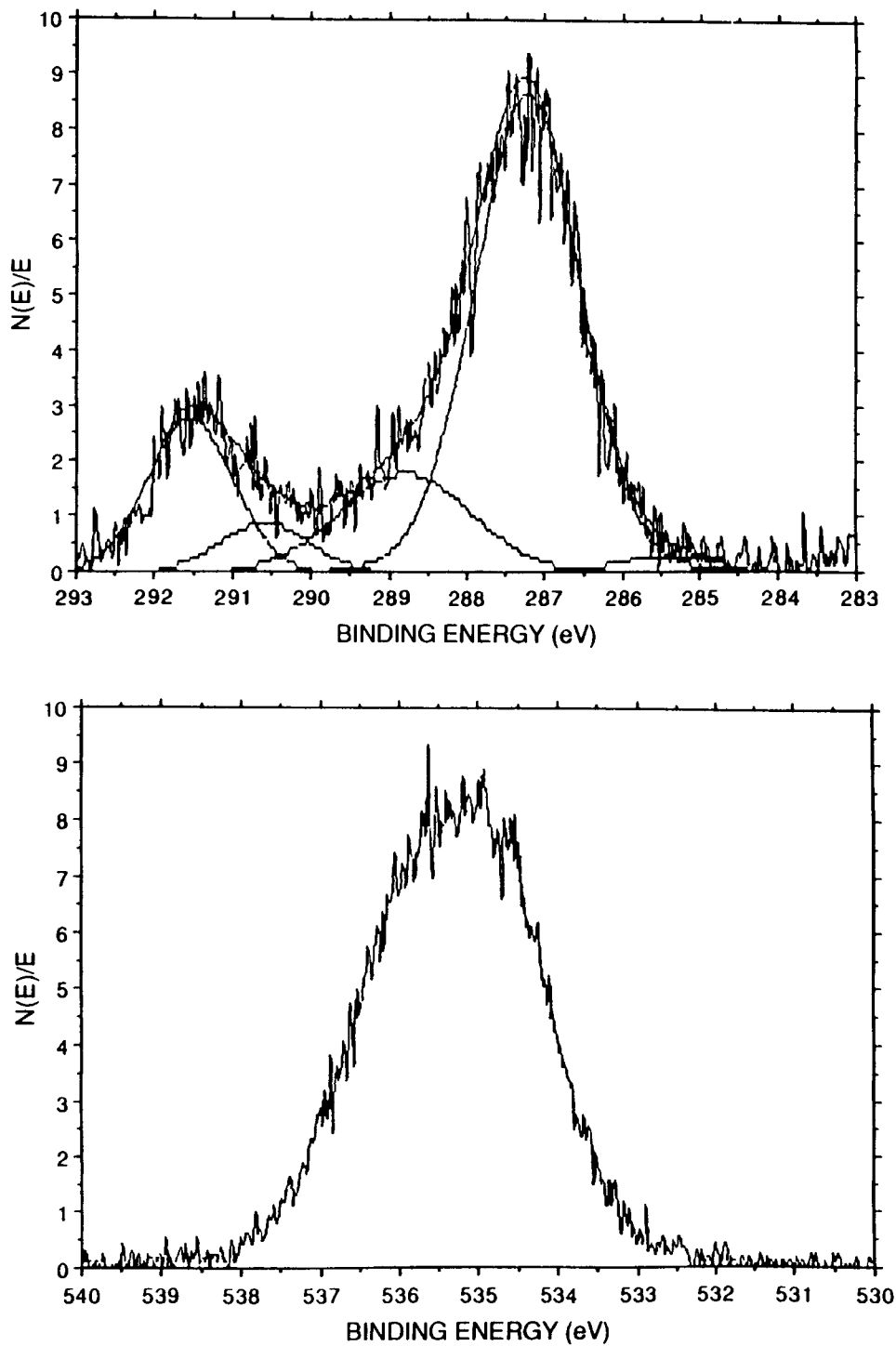


**Figure 3** ESCA multiplex spectra from the acrylic acid plasma polymer deposited on LDPE (immediately after 50 W plasma polymerization for 10 min) at a takeoff angle = 45°: (i) C<sub>1s</sub>; (ii) O<sub>1s</sub>.

gradient centrifugation in HEPES-Tyroses buffer solution of pH 7.3 by a modification of Walsh and Griffin's method.<sup>22,23</sup>

Plasma-modified LDPE surfaces were cut into 3 × 3 mm-square samples and equilibrated in the HEPES-Tyroses buffer solution (with bovine serum

albumin [BSA]) on a polystyrene Petri dish for about 1 h. Then, the samples were covered by a layer of washed platelet suspension ( $\approx 200,000$  platelets per  $\mu\text{L}$ ) for platelet adhesion and spreading in a  $37^\circ\text{C}$  incubator with  $\text{CO}_2$  flow. After 5 min, the washed platelet suspension was rinsed off and the samples were covered by Hepes-Tyroses buffer solution (with BSA). The samples were then placed in the  $37^\circ\text{C}$   $\text{CO}_2$  incubator for another 40 min to allow further spreading of the adhered platelets. After a total of 45 min incubation in  $\text{CO}_2$ , the adhered platelets were fixed in 2 vol % glutaldehyde in a Hepes solution for 30 min. After glutaldehyde fixation, the samples were dehydrated with ethanol and finally in a  $\text{CO}_2$  critical point drying apparatus (Tousimis Autosamdri 814). The samples were kept in a desiccator to avoid moisture from the atmosphere. Scanning electron microscopy, at a 15 kV accelerating voltage, was used to observe the platelet shape change, shape change distribution, and the total number density of the adhering canine platelets.

## RESULTS AND DISCUSSION

### ESCA

Angle-dependent ESCA survey and multiplex spectra were collected to study the surface elemental compositions of the acrylic acid and allylamine plasma polymers as a function of depth and time. Carbon (C) and oxygen (O) were the only two elements present on the acrylic acid plasma polymer sample surfaces as revealed by the ESCA survey scan. Carbon (C), nitrogen (N), and oxygen (O) were found on the allylamine plasma polymers' surfaces.

ESCA results indicated that there was a large amount of oxygen incorporated in the plasma polymer films formed by acrylic acid plasma polymerization (80–87 atm %) (Table I). By plotting the O/C atomic concentration ratio vs. the sine of the takeoff angle ( $\sin \theta$ ), the relative atomic concentration depth profiles in the top 100 Å of the plasma polymer could be determined (Fig. 2). The plot clearly indicates that a larger amount of oxygen was incorporated when a low plasma energy was applied. Immediately after the plasma deposition, maximum oxygen atomic concentrations were observed in the data taken at  $\theta = 45^\circ$ . However, 6 days after the plasma polymerization, the oxygen-containing functional groups diffused toward the bulk of the material and the maxima shifted into the bulk.<sup>24–27</sup>

There was 20 atm % C and 80 atm % O right after the 50 W acrylic acid plasma polymerization, which changed to 24 atm % C and 76 atm % O 6 days afterward. In the deconvolution of the  $\text{C}_{1s}$  peak, Figure 3(i) shows the relative amounts of different functional groups in the 20 atm % carbon of the 50 W acrylic acid plasma polymer: 16%  $-\text{C}(\text{O})\text{OH}$ , 6%  $>\text{C}=\text{O}$ , 16%  $\equiv\text{C}-\text{OH}$ , 61%  $>\text{CH}_2$  (aliphatic carbon), and 2% C (graphitic carbon). Six days after the plasma deposition, the functional group composition of the 24 atm % carbon changed to 18%  $-\text{C}(\text{O})\text{OH}$ , 4%  $>\text{C}=\text{O}$ , 14%  $\equiv\text{C}-\text{OH}$ , 61%  $>\text{CH}_2$ , and 2% C. Surprisingly, the  $-\text{C}(\text{O})\text{OH}$  group concentration increased in the surface region from 16% of the 20 atm % carbon (= 3 atm %) immediately after the 50 W acrylic acid plasma polymerization to 18% of the 24 atm % carbon (= 4 atm %) 6 days afterward. This was most likely due

**Table II** ESCA Results for the Allylamine Plasma Polymer Deposited on LDPE

Takeoff Angle (Degrees)	Atomic Concentration (%)					
	Immediately after Plasma Polymerization			7 Days after Plasma Polymerization		
	C	O	N	C	O	N
5 W						
10	37.67	16.13	46.20	37.60	36.96	25.44
30	31.54	21.01	47.45	38.26	30.91	30.83
45	36.27	16.99	46.73	32.35	35.19	32.46
75	37.37	11.77	50.87	39.20	24.40	36.39
10 W						
10	41.17	34.43	24.40	35.65	43.70	20.65
30	38.05	27.94	34.01	38.15	35.84	26.01
45	38.58	27.61	33.81	32.27	40.88	26.85
75	40.77	13.74	45.49	34.82	37.70	27.48
30 W						
10	30.34	37.31	32.35	36.02	40.49	23.49
30	29.60	35.61	34.79	34.21	38.13	27.66
45	34.97	30.89	34.14	30.75	41.52	27.73
75	39.73	12.78	47.49	33.84	37.97	28.19
50 W						
10	43.62	21.60	34.77	32.11	42.71	25.19
30	34.83	23.29	41.88	29.28	42.92	27.81
45	41.47	20.97	37.56	27.26	44.32	28.42
75	36.85	14.26	48.89	33.58	33.90	32.53

to the post-plasma-oxidation of the surface reactive sites and entrapped reactive species by atmospheric oxygen.

High-resolution ESCA multiplex scans of  $C_{1s}$ ,  $N_{1s}$ , and  $O_{1s}$  peaks were used to obtain quantitative results for the elemental and functional group compositions of the allylamine plasma polymers.<sup>12</sup> There was 34–47 atm % nitrogen and 17–31 atm % oxygen in the allylamine plasma polymer (Table II). There were two possible ways for the oxygen to become incorporated in both plasma treatments: (i) adventitious oxygen present in the plasma reactor during plasma reaction and (ii) post-plasma-treatment reaction with atmospheric oxygen.<sup>1,15</sup> The 5 W plasma energy produced a film with the largest amount of nitrogen incorporation, the 10 W plasma yielded the least, and the 30 and 50 W plasmas were about the same. Maximum nitrogen concentrations were observed in the data taken at  $\theta = 30^\circ$ . After 7 days, the maxima shifted to  $\theta = 45^\circ$  and had smaller magnitudes. The detection of these transient maxima was probably due to the migration of the hydrophilic nitrogen-containing functional groups from the surface regions into the bulk of the material. As a

result, the location of the maximum nitrogen concentrations moved into the bulk of the material and decreased in magnitude with time. The different nitrogen concentrations in the thin films polymerized at various plasma energies were due to the different compositions of the plasmas. At high energy, the plasma contains more fragmented species than at low energy. Therefore,  $50 > 30 > 10$  W in the N/C atomic concentration ratios in the formation of the allylamine plasma polymers (Fig. 4). The extraordinary high N/C atomic concentration ratio of the 5 W plasma polymer was probably due to the low plasma energy, which was only capable of producing small nitrogen-rich reactive species that had high reactivity in the formation of the thin film. Since the high-energy plasma had more allylamine fragments, the plasma polymer was more highly cross-linked. This can rationalize the difference in N/C atomic concentration ratios 7 days after the plasma polymerization:  $50 \approx 5 > 30 > 10$  W. The diffusivities of the nitrogen-containing functional groups were probably lower in the more highly cross-linked network produced by the 50 W allylamine plasma.

The 30 W allylamine plasma polymer had the

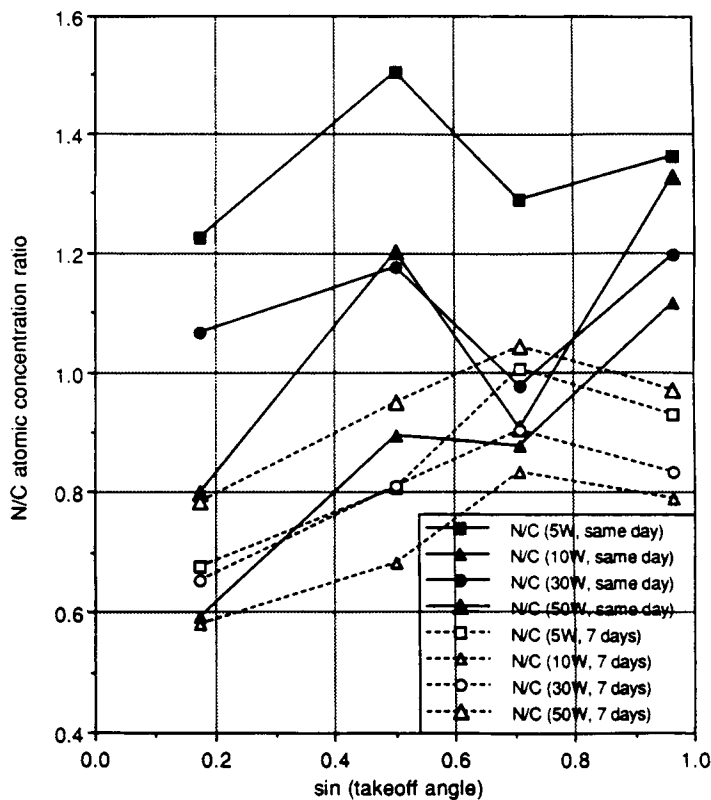


**Figure 4** N/C atomic concentration ratio vs.  $\sin \theta$  for the allylamine plasma polymer deposited on LDPE (10 min).

largest oxygen content in its surface region, the 10 W plasma polymer had less, and the 5 and 50 W plasma polymers had the least. This was because the high-energy plasma contained more fragmented oxygen-rich reactive species that could be incorporated into the thin film. However, the oxygen-rich species also have strong etching characteristics. Therefore, in the 50 W plasma, the etching by these oxygen-rich species had a strong effect on the thin-film formation and its plasma polymer had less oxygen-containing functional groups than the 30 and 10 W plasma polymers. Seven days after the plasma polymerization, the O/C ratios varied as follows: 50 > 30 > 10 > 5 W (Fig. 5). In addition, the oxygen concentration of the plasma polymers was higher 7 days after the plasma polymerization than immediately after the plasma polymerization. This was probably due to the higher amounts of reactive sites and entrapped reactive species in the high-energy plasma polymers. The post-plasma-treatment reaction of the high-energy plasma polymer with the atmospheric oxygen took place to a larger extent than that on the low-energy plasma polymer. As an

example in the allylamine plasma polymers, the  $\theta = 45^\circ$  data of the 5 W allylamine plasma polymer (Fig. 6) showed that the 36 atm % carbon consisted of 2% C(O)OH, 2%  $>N-C=O$ , 6%  $>C=O$ , 9% C—O, 27% C—N, 51%  $>CH_2$ , and 3% C and that the 47 atm % nitrogen consisted of 3%  $NO_2$ , 3% NO, 91%  $NH_2$ , 2% NH, and 1%  $C\equiv N$ . There was also 17 atm % oxygen on the surface. Seven days after the plasma polymerization, its composition changed to 32 atm % carbon [4% C(O)OH, 3%  $>N-C=O$ , 7%  $>C=O$ , 9% C—O, 18% C—N, 56%  $>CH_2$ , and 3% C], 33 atm % nitrogen (1%  $NO_2$ , 1% NO, 93%  $NH_2$ , 2% NH, and 3%  $C\equiv N$ ), and 35 atm % oxygen.

#### ATR-FTIR

Figures 7 and 8 show the ATR-FTIR spectra of the 10 W acrylic acid and 50 W allylamine plasma polymers. Because of the nonuniformity of film deposition, quantitative comparison of the functionalities produced at different plasma excitation energies was unsuccessful. Only qualitative results (i.e., types of

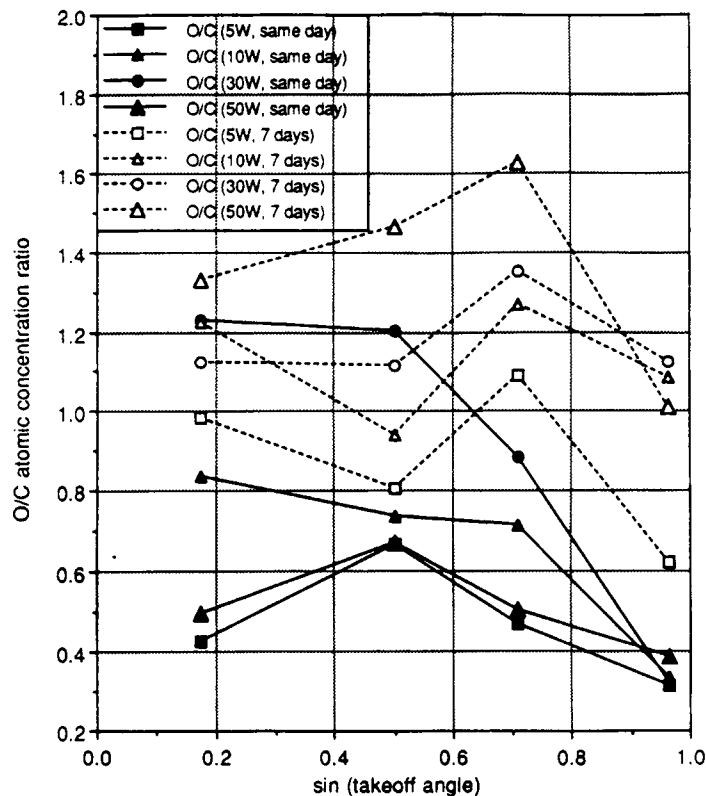


**Figure 5** O/C atomic concentration ratio vs.  $\sin \theta$  for the allylamine plasma polymer deposited on LDPE (10 min).



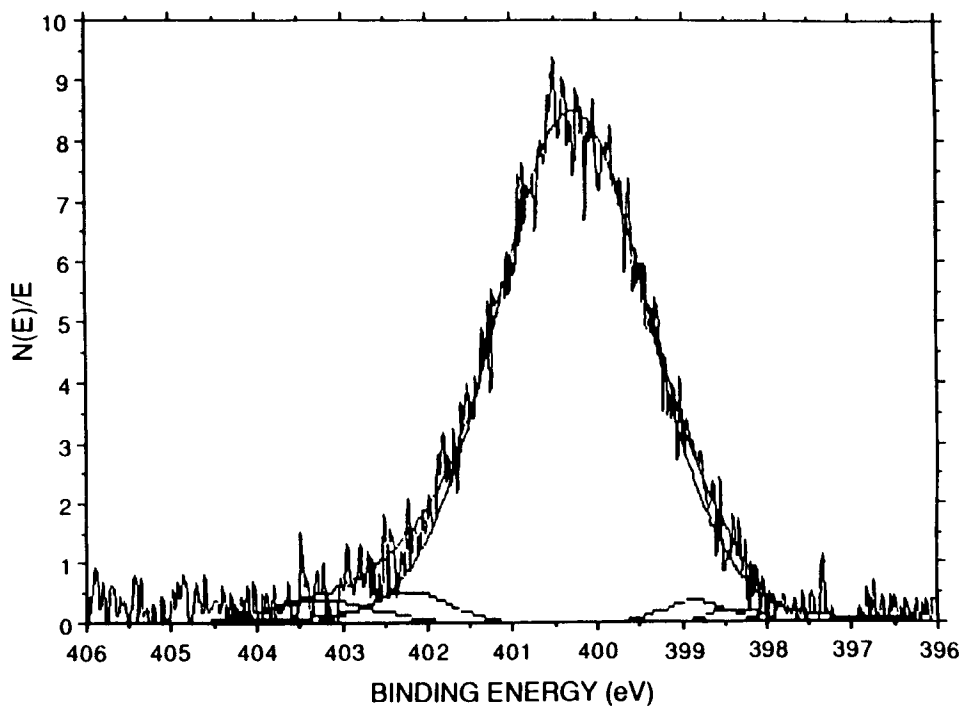
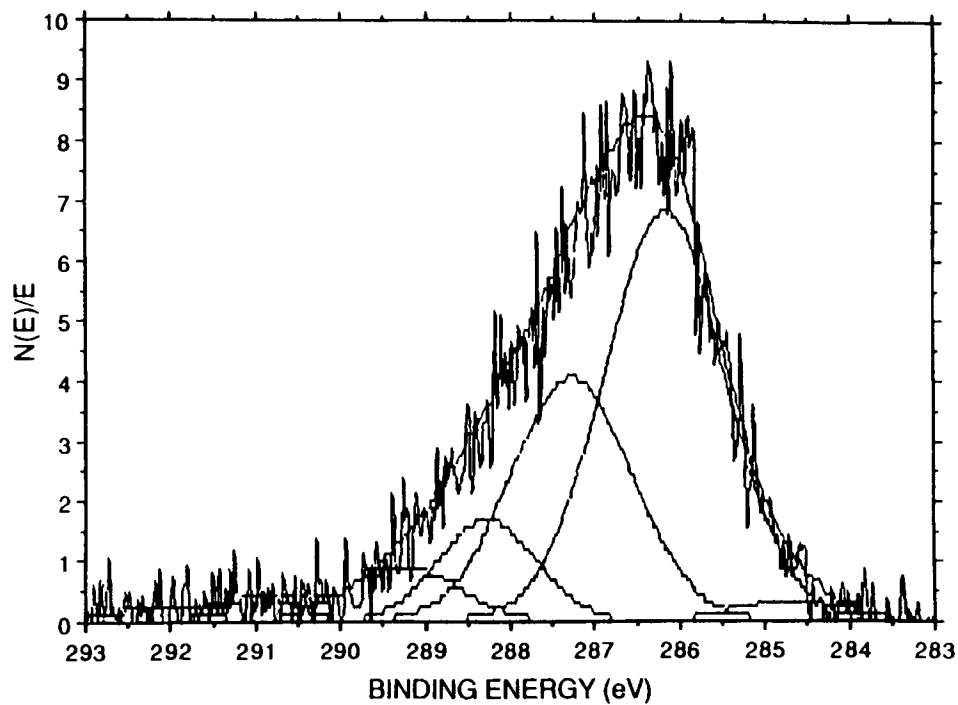


**Figure 6** ESCA multiplex spectra from the allylamine plasma polymer deposited on LDPE (immediately after 5 W plasma polymerization for 10 min) at a takeoff angle =  $45^\circ$ : (i)  $C_{1s}$ ; (ii)  $N_{1s}$ .

functional groups) were obtained. Figure 7 shows that C—H ( $\nu = 2935 \text{ cm}^{-1}$ ), C—O ( $\nu = 1238, 1176, 1044, 919 \text{ cm}^{-1}$ ), O—H ( $\nu = 2635, 1451, 1414 \text{ cm}^{-1}$ ),

and C=O ( $\nu = 1696 \text{ cm}^{-1}$ ) groups were formed by the plasma polymerization of acrylic acid.

Qualitative results indicated that plasma poly-

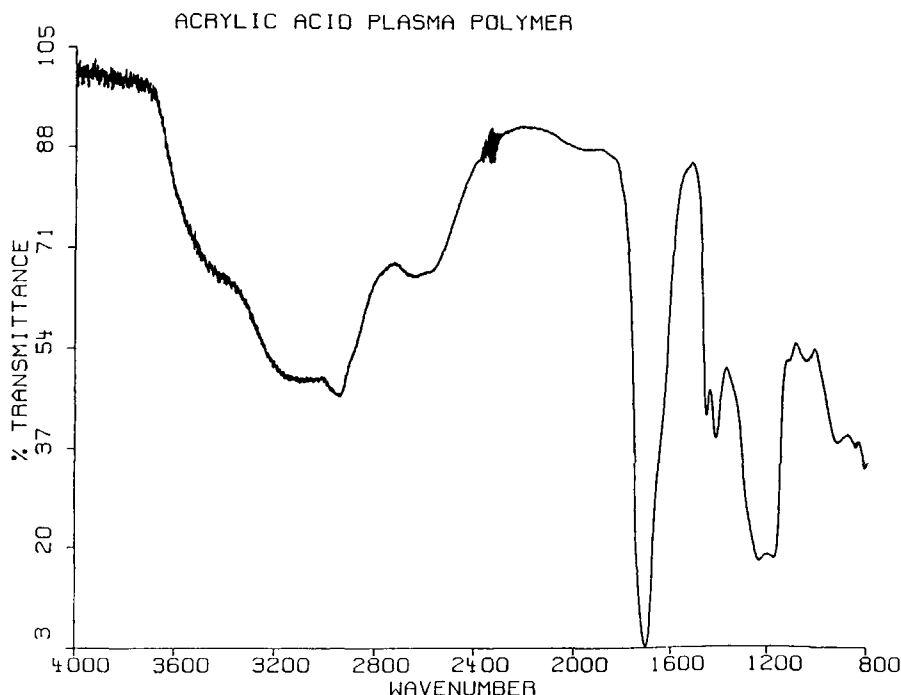


**Figure 7** ATR-FTIR spectrum for the acrylic acid plasma polymer formed at 10 W for 30 min. The acrylic acid plasma polymer was deposited on a Ge IRE. This ATR-FTIR difference spectrum of the plasma polymer is obtained after the subtraction of the IRE background spectrum from the sample spectrum. Similar ATR-FTIR spectra were obtained for plasma polymerization of acrylic acid at 30 and 50 W. The peaks are located at the same wavenumbers but have slightly different intensities.

merization of allylamine at different plasma energies yielded the same types of functional groups.<sup>12</sup> Figure 8 shows that NH ( $\nu = 3223 \text{ cm}^{-1}$ ),  $\text{NH}_2$  ( $\nu = 3223, 850 \text{ cm}^{-1}$ ),  $\text{C}\equiv\text{N}$  ( $\nu = 2146 \text{ cm}^{-1}$ ),  $\text{C}=\text{N}$  ( $\nu = 1652 \text{ cm}^{-1}$ ),  $\text{C}-\text{N}$  ( $\nu = 1088 \text{ cm}^{-1}$ ), CH ( $\nu = 1458 \text{ cm}^{-1}$ ),  $\text{CH}_2$  ( $\nu = 1414 \text{ cm}^{-1}$ ),  $\text{CH}_3$  ( $\nu = 1370 \text{ cm}^{-1}$ ),  $\text{C}=\text{O}$  ( $\nu = 1652 \text{ cm}^{-1}$ ),  $\text{C}-\text{O}$  ( $\nu = 1088 \text{ cm}^{-1}$ ),  $\text{O}-\text{H}$  ( $\nu = 3335, 2960, 1370 \text{ cm}^{-1}$ ), and  $\text{N}-\text{O}$  ( $\nu = 1652, 1458, 806 \text{ cm}^{-1}$ ) were found in the plasma-polymerized allylamine.

### Contact Angle

Air and *n*-octane static sessile drop contact angles were measured for the plasma-polymerized acrylic acid and allylamine deposited on the LDPE substrates through the water medium (Tables III and IV). Air in water contact angles ( $\theta_{\text{air/water}}$ ) changed from  $86^\circ$  before the plasma reaction to an average of  $32^\circ$  after acrylic acid plasma polymerization and to an average of  $40^\circ$  after allylamine plasma polymerization. Octane in water contact angles ( $\theta_{\text{octane/water}}$ ) changed from  $180^\circ$  (wetting) to an av-

erage of  $65^\circ$  after acrylic acid plasma polymerization and to an average of  $61^\circ$  after allylamine plasma polymerization. Nine days after the acrylic acid plasma polymerization,  $\theta_{\text{air/water}}$  increased to an average of  $37^\circ$  and  $\theta_{\text{octane/water}}$  increased to an average of  $70^\circ$ . Seven days after the allylamine plasma polymerization,  $\theta_{\text{air/water}}$  further decreased to an average of  $28^\circ$  and  $\theta_{\text{octane/water}}$  decreased to an average of  $40^\circ$ . The decreases in both the air and octane in water contact angles after the plasma treatments were due to the formation of the hydrophilic oxygen-containing and nitrogen-containing functional groups on the substrate surfaces.<sup>15,25-27</sup> These functional groups diffused into the bulk of the material with time since the air/substrate interface is hydrophobic.<sup>15,18,27</sup> This is the reason for the increase in the air and octane contact angles on the acrylic acid plasma polymers 9 days after the plasma polymer formation (Fig. 9).<sup>18,25,26</sup> However, for the allylamine plasma polymers, there was a large extent of post-plasma-treatment reaction with atmospheric oxygen (see Table II). As a result, there were large amounts of hydrophilic oxygen-containing functionalities created on the plasma polymer surfaces after the plasma

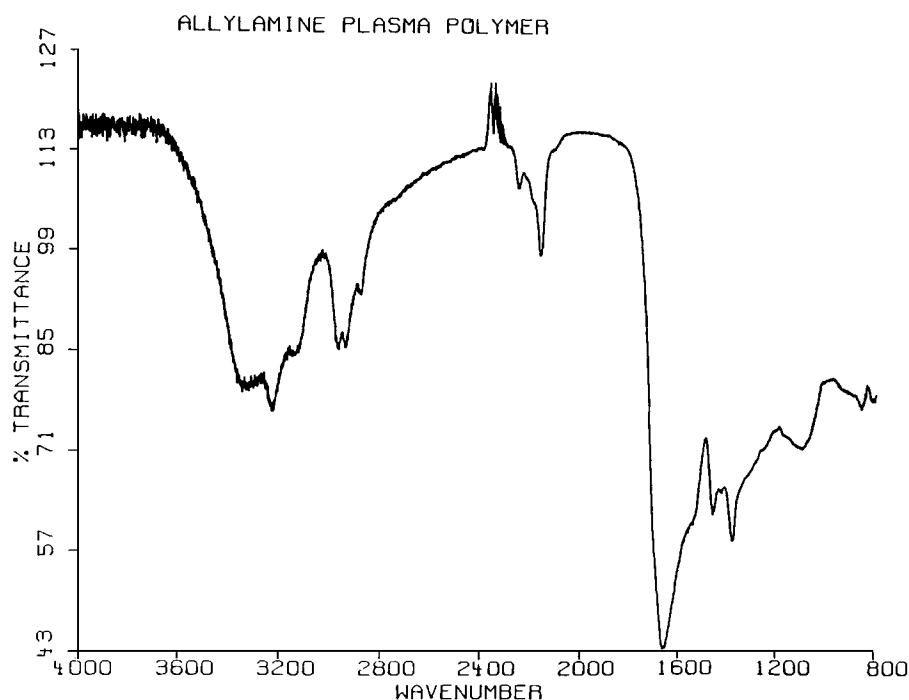


**Figure 8** ATR-FTIR spectrum for the allylamine plasma polymer formed at 50 W for 30 min. The allylamine plasma polymer was deposited on a Ge IRE. Similar ATR-FTIR spectra were obtained for plasma polymerization of allylamine at 5, 10, and 30 W. The peaks are located at the same wavenumbers but have slightly different intensities.

polymerization. The contact angles of the allylamine plasma polymers therefore decreased further 7 days after the allylamine plasma polymerization (Fig. 10).

There was no difference in contact angles for allylamine plasma polymers treated at different plasma energy levels. The rather constant surface hydrophilicity of all samples treated at different plasma energies might be because there was about

the same total amount of nitrogen-containing and oxygen-containing hydrophilic functional groups formed on the surfaces at all the energies used for the plasma treatments (see Table II). In contrast, the 10 W acrylic acid plasma polymer had smaller air and octane contact angles because of its higher content of hydrophilic oxygen-containing functional groups compared to the acrylic acid plasma polymers

**Table III** Air and Octane in Water Contact Angles for the Acrylic Acid Plasma Polymer Deposited on LDPE

Plasma Energy (W)	Contact Angle (Degrees)			
	Immediately after Plasma Polymerization		9 Days after Plasma Polymerization	
	Air	Octane	Air	Octane
0 (Untreated)	86 ± 3	180 ± 0	86 ± 3	180 ± 0
10	22 ± 3	57 ± 5	30 ± 2	65 ± 2
30	39 ± 3	64 ± 4	43 ± 5	71 ± 4
50	35 ± 4	75 ± 3	37 ± 4	75 ± 4

**Table IV** Air and Octane in Water Contact Angles for the Allylamine Plasma Polymer Deposited on LDPE

Plasma Energy (W)	Contact Angle (Degrees)			
	Immediately after Plasma Polymerization		7 Days after Plasma Polymerization	
	Air	Octane	Air	Octane
0 (Untreated)	86 ± 3	180 ± 0	86 ± 3	180 ± 0
5	39 ± 5	61 ± 6	29 ± 4	37 ± 7
10	38 ± 5	60 ± 5	29 ± 3	37 ± 3
30	43 ± 6	63 ± 5	26 ± 2	43 ± 3
50	39 ± 7	61 ± 4	26 ± 4	44 ± 5

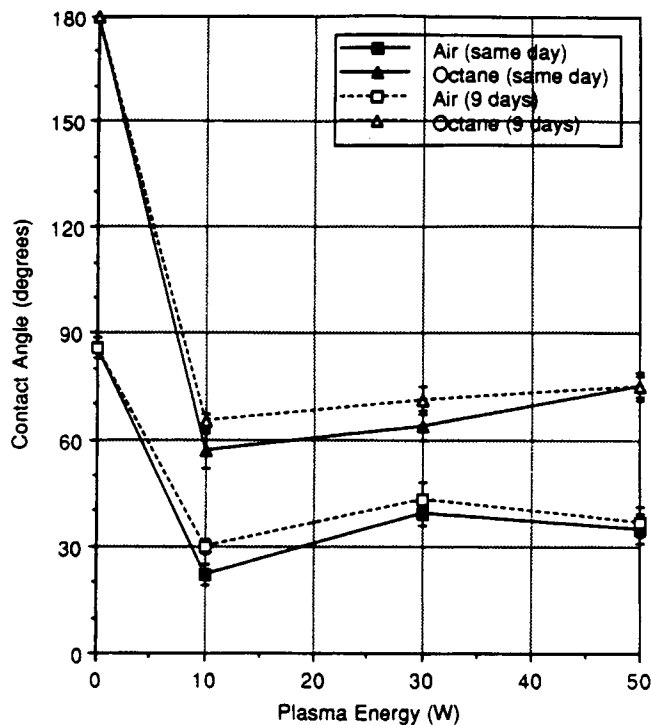


**Figure 9** Air and octane in water contact angles for the acrylic acid plasma polymer deposited on LDPE.

formed at higher energy levels. The different surface morphologies of the allylamine plasma polymers formed in different plasma energies (see Fig. 14) did

not seem to have a major effect on the contact-angle measurements. This was probably due to the small scale of the surface roughness.

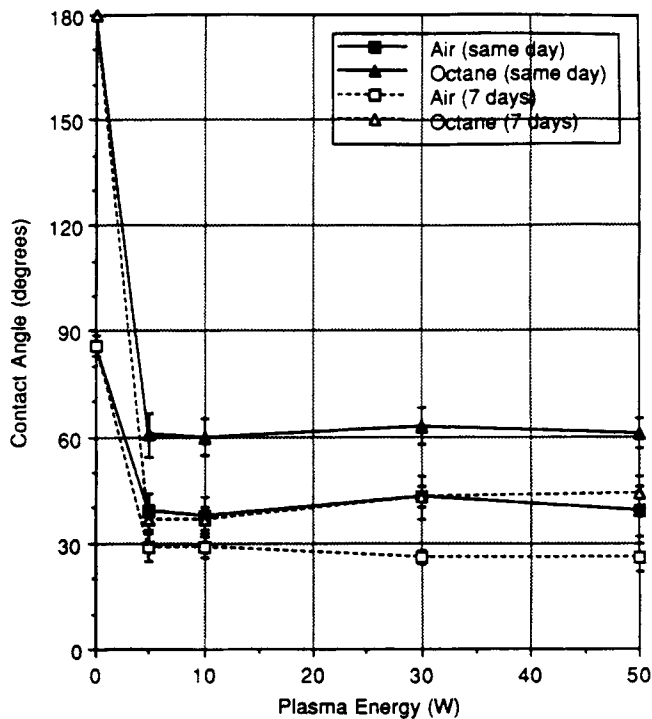


**Figure 10** Air and octane in water contact angles for the allylamine plasma polymer deposited on LDPE.

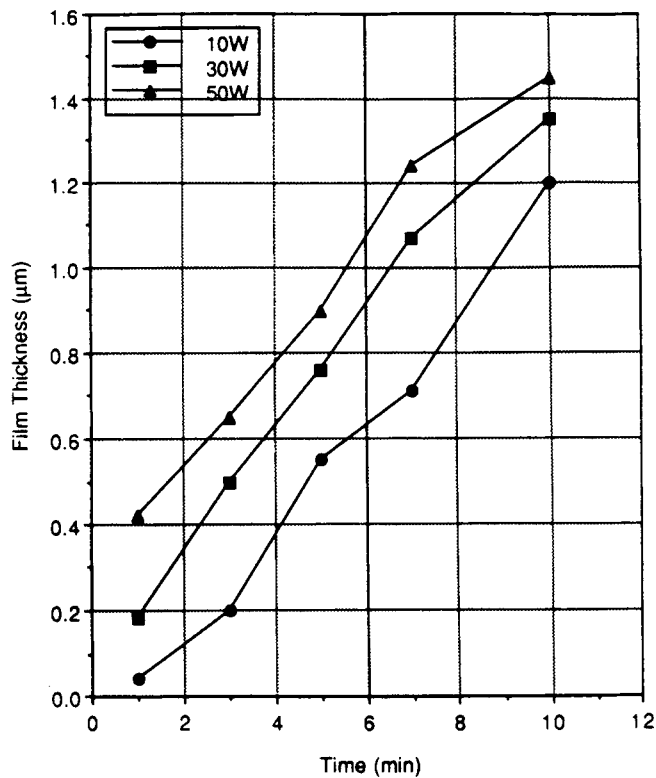


Figure 11 Acrylic acid plasma polymer deposition rates.

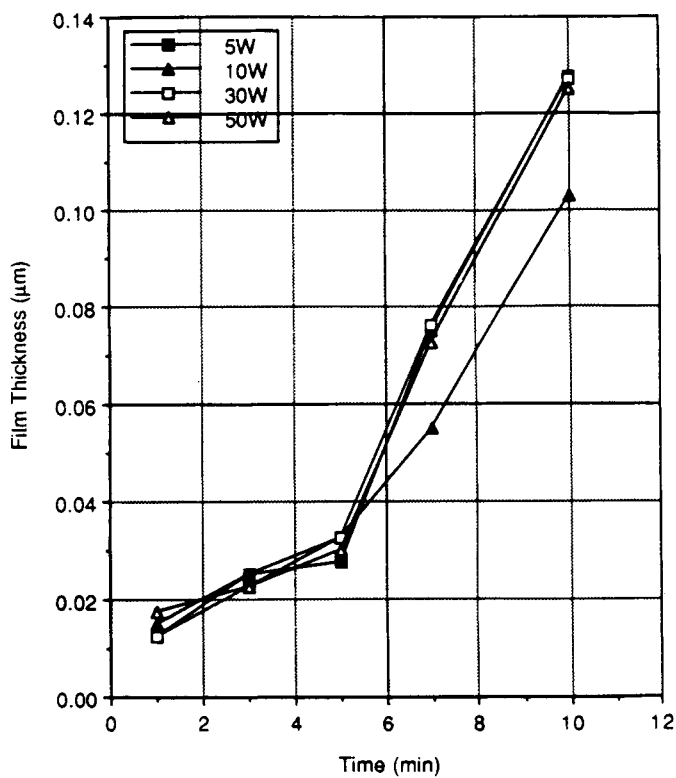







Figure 12 Allylamine plasma polymer deposition rates.

**Table V Five Stages of Platelet Morphological Changes upon Adhesion to Foreign Surfaces**

	Stage	Morphology Description
	Round	Round or discoid, no pseudopodia present
	Dendritic	Early pseudopodial, no flattening evident
	Spread-dendritic	Intermediate pseudopodial, one or more pseudopodia flattened, hyaloplasm not spread between pseudopodia
	Spreading	Late pseudopodial, hyaloplasm spreading
	Fully spread	Hyaloplasm well spread, no distinct pseudopodia

**Profilometry**

Figure 11 shows that the deposition rates for acrylic acid plasma polymers were fairly linear and about the same ( $d_{AAc} = 0.13 \mu\text{m min}^{-1}$ ) for all three plasma

energy levels except the initial deposition rates, i.e., at the time when the plasma was in direct contact with the substrate surface. The initial deposition rate was the highest for the 50 W acrylic acid plasma ( $d_{0,AAc(50W)} = 0.42 \mu\text{m min}^{-1}$ ) and lower for the 30

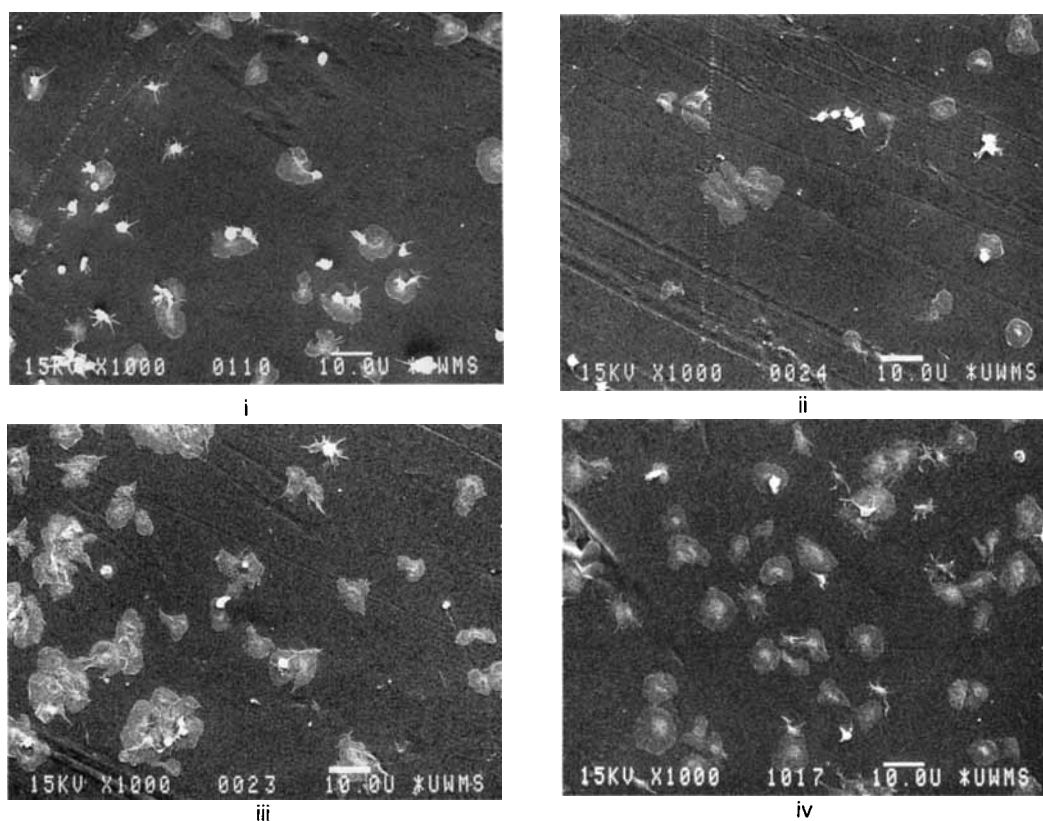


**Figure 13** Canine platelet adhesion to the acrylic acid plasma polymer deposited on LDPE (10 min): (i) untreated, (ii) 10 W; (iii) 30 W; (iv) 50 W.

W ( $d_{0,AAc(30W)} = 0.19 \mu\text{m min}^{-1}$ ) and 10 W ( $d_{0,AAc(10W)} = 0.04 \mu\text{m min}^{-1}$ ) plasmas. Figure 12 shows that the deposition rates for the allylamine plasma polymers ( $d_{AAm}$ ) were the same for all four different plasma energy levels. The initial deposition rate ( $d_{0,AAm}$ ) was  $14 \text{ nm min}^{-1}$ . A small degree of nonlinearity in the deposition rate was observed at about 5 min. Possibly, the substrate-glass surface chemistry or surface tension influenced the early deposition rates. From  $t = 1 \text{ min}$  to  $t = 5 \text{ min}$ , the allylamine plasma polymer deposition rate was approximately  $3.8 \text{ nm min}^{-1}$ , and from  $t = 5 \text{ min}$  to  $t = 10 \text{ min}$ , the second deposition rate was about 19

$\text{nm min}^{-1}$ . These results revealed that the plasma polymer deposition rate of acrylic acid was about seven times that of allylamine under the same gas flow conditions.

### Platelet Adhesion

Canine platelet adhesion experiments were carried out for both the acrylic acid and allylamine plasma-treated LDPE to test their blood biocompatibility. Table V shows the somewhat arbitrary classification of the five stages of shape change for activated platelets.<sup>28</sup> Initially, an unactivated platelet has a

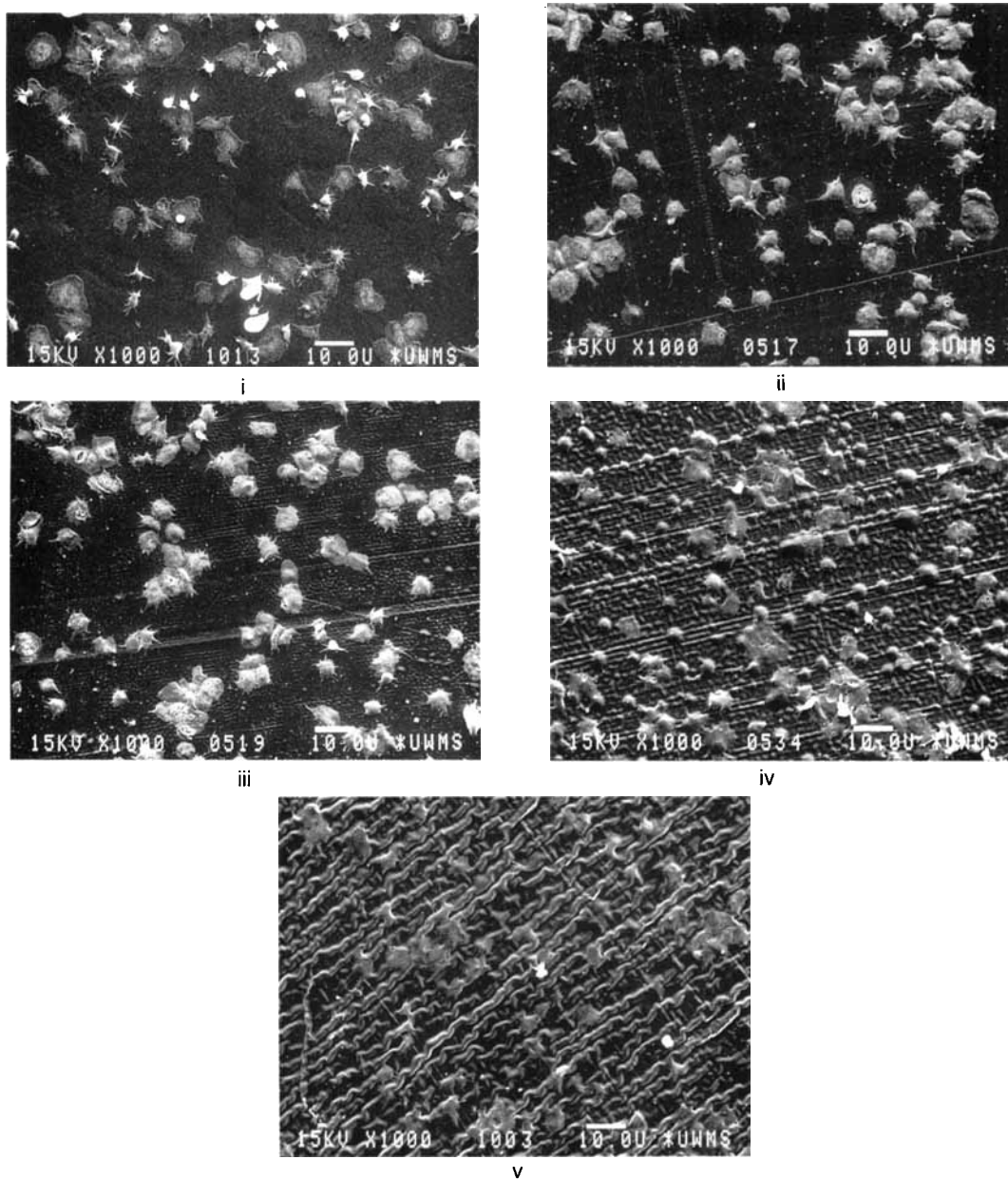


**Figure 14** Canine platelet adhesion to the allylamine plasma polymer deposited on LDPE (10 min): (i) untreated; (ii) 5 W; (iii) 10 W; (iv) 30 W; (v) 50 W.

round or discoid shape. Sometimes, a few pseudopods are extruded (dendritic shape) and retracted from a platelet dependent on whether or not it is activated. An activated platelet will go on to spread in an irreversible process. When the activated platelet begins to spread, the cell becomes flatter and loses its rigidity and acquires a spread-dendritic shape. The contents of the cell move outward between the pseudopods (spreading shape). Eventually, the platelet reaches a fully spread shape. Figures 13 and 14 are typical SEM micrographs showing the platelet density and morphology on the acrylic acid and allylamine plasma-treated samples. Tables VI and VII and Figures 15 and 16 show the statistics of the platelet-shape distributions. The acrylic acid plasma-treated surfaces appeared smooth (Fig. 13) and independent of plasma excitation energy. There were more dendritic platelets but less spread-dendritic and fully spread platelets adhering to the acrylic acid plasma polymer films formed on LDPE than on the untreated LDPE.<sup>6-8</sup> The acrylic acid plasma polymer films were therefore less thrombogenic than were the LDPE substrates. In addition, the 10 and 30 W acrylic acid plasma polymers were more thromboresistant than the 50 W plasma polymer. In fact, the platelet adhesion characteristics of the 50 W acrylic acid plasma polymer was very similar to that of the untreated LDPE. The platelet adhesion density of the 10 W acrylic acid plasma polymer was 2.7 platelets per 1000  $\mu\text{m}^2$  (8% round, 13% dendritic, 10% spread-dendritic, 24% spreading, and 45% fully spread); the platelet adhesion density of the control untreated LDPE substrate was 6.2 platelets per 1000  $\mu\text{m}^2$  (2% round, 2% dendritic, 14% spread-dendritic, 12% spreading, and 70% fully spread). Since the acrylic acid plasma treatment resulted in a larger amount of the oxygen-containing functional group incorporation at low plasma energy

levels (Table I), the acidic hydrophilic oxygen-containing functional groups might have a significant role in preventing platelet adhesion and platelet spreading.

Allylamine plasma treatment of LDPE had a negative effect on blood thromboresistance (Table VII and Fig. 14).<sup>8,11,29</sup> General observation of the SEM micrographs (Fig. 14) shows that different surface morphologies were generated on surfaces where allylamine was polymerized at different plasma energy levels. Surface roughness increased with increasing plasma energies, i.e., 50 > 30 > 10 > 5 > untreated LDPE. Because of the low contrast of the surface irregularities and the adhered platelets, it was not possible to count the exact numbers of different platelet shapes for the platelets adhering to the allylamine plasma polymerized at 30 and 50 W. The platelet adhesion density was the same on the 5 and 10 W plasma-polymerized allylamine (10.3 platelets per 1000  $\mu\text{m}^2$ ) which was higher than that on untreated LDPE (8.3 platelets per 1000  $\mu\text{m}^2$ ). Furthermore, there were larger percentages of spreading and fully spread platelets adhering to the allylamine plasma polymers (1% round, 2% dendritic, 11% spread-dendritic, 33% spreading, and 54% fully spread) than to the untreated LDPE (2% round, 22% dendritic, 27% spread-dendritic, 13% spreading, and 36% fully spread). Rough estimates from observation of the SEM micrographs indicate that there was about the same platelet adhesion density on the 30 W plasma-polymerized allylamine thin film as on the 5 and 10 W allylamine plasma polymer thin films; however, the 50 W allylamine plasma polymer might have slightly fewer platelets adhering to its surface. Most of the platelets adhering to the 50 W allylamine plasma polymer were fully spread, but many of the platelets adhering to the 30 W allylamine plasma polymer were spread-

**Table VI Platelet Shape Distributions of Canine Platelets Adhering to the Acrylic Acid Plasma Polymer Deposited on LDPE**

Platelet Shape	Platelet Counts at Various Plasma Energy Treatments (Platelets, #/1000 $\mu\text{m}^2$ )			
	Untreated	10 W	30 W	50 W
Round (R)	0.2 ± 0.1	0.2 ± 0.2	0.3 ± 0.2	0.2 ± 0.1
Dendritic (D)	0.1 ± 0.1	0.4 ± 0.2	0.5 ± 0.2	0.2 ± 0.2
Spread-dendritic (SD)	0.8 ± 0.2	0.3 ± 0.1	0.5 ± 0.1	0.6 ± 0.2
Spreading (S)	0.8 ± 0.2	0.6 ± 0.2	0.8 ± 0.2	1.2 ± 0.2
Fully spread (FS)	4.3 ± 0.3	1.2 ± 0.3	2.9 ± 0.4	3.7 ± 0.9
Total	6.2 ± 0.8	2.7 ± 1.0	5.0 ± 1.1	5.9 ± 1.6



**Table VII Platelet Shape Distributions of Canine Platelets Adhering to the Allylamine Plasma Polymer Deposited on LDPE**

Platelet Shape	Platelet Counts at Various Plasma Energy Treatments (Platelets, #/1000 $\mu\text{m}^2$ )		
	Untreated	5 W	10 W
Round (R)	$0.2 \pm 0.1$	$0.1 \pm 0.1$	$0.1 \pm 0.1$
Dendritic (D)	$1.8 \pm 0.6$	$0.2 \pm 0.2$	$0.2 \pm 0.5$
Spread-dendritic (SD)	$2.2 \pm 0.7$	$1.2 \pm 0.5$	$1.5 \pm 0.4$
Spreading (S)	$1.1 \pm 0.3$	$3.3 \pm 0.6$	$3.3 \pm 0.5$
Fully spread (FS)	$3.0 \pm 0.7$	$5.5 \pm 1.2$	$5.6 \pm 1.2$
Total	$8.3 \pm 2.4$	$10.2 \pm 2.5$	$10.4 \pm 2.7$

dendritic. The surface roughness of the 50 W allylamine plasma polymer might have played a significant role in activating the adhering platelets. In contrast to the platelet adhesion characteristics on the acidic acrylic acid plasma polymer surfaces, the basic allylamine plasma polymers were much more thrombogenic in terms of platelet adhesion number density and platelet spreading.

### SUMMARY

Acidic oxygen-containing functional groups were incorporated onto LDPE substrates by acrylic acid [ $\text{CH}_2=\text{CHC}(\text{O})\text{OH}$ ] plasma polymerization. ESCA, ATR-FTIR spectroscopy, static contact-angle measurements, and SEM were used to characterize the modified LDPE surfaces. Low plasma en-

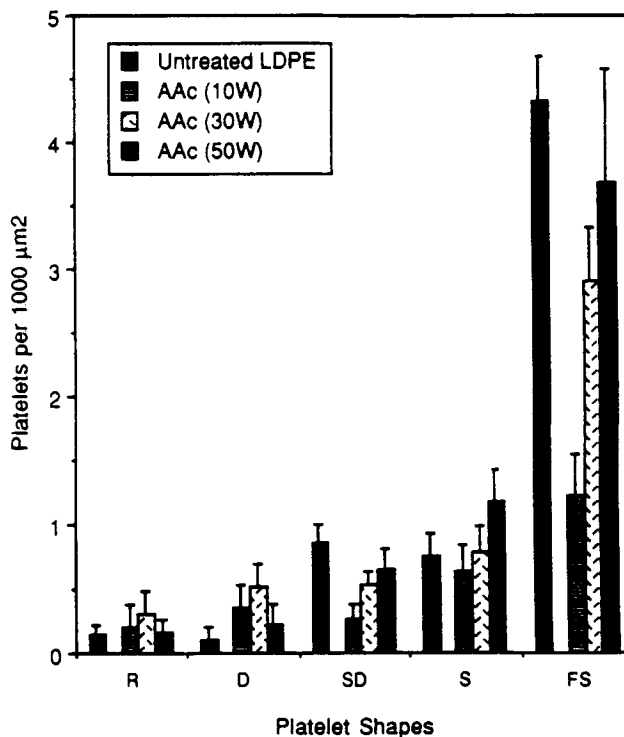


**Figure 15** Platelet shape distributions of canine platelets adhering to the acrylic acid plasma polymer deposited on LDPE. Platelet shapes: R, round; D, dendritic; SD, spread-dendritic; S, spreading; FS, fully spread.

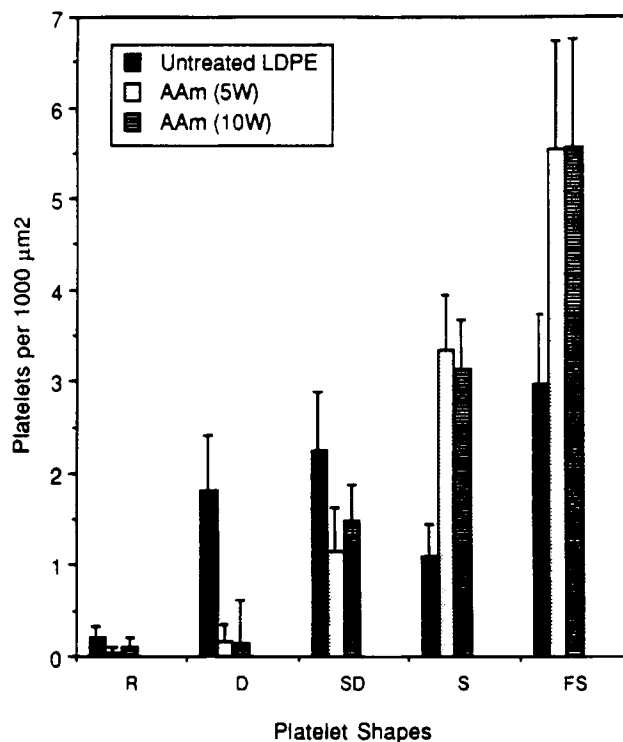


**Figure 16** Platelet shape distributions of canine platelets adhering to the allylamine plasma polymer deposited on LDPE. Platelet shapes: same as in Figure 15 legend.

ergy levels (such as 10 W) produced films containing larger amounts of oxygen-containing functional groups. ESCA and contact-angle experiments showed that the hydrophilic oxygen-containing functional groups diffused away from the surface region of the plasma-treated LDPE with time. The acrylic acid plasma polymers were less thrombogenic in terms of platelet adhesion and platelet spreading than the untreated LDPE surface. The acrylic acid plasma polymers formed at low plasma energies (10 and 30 W) were more thromboresistant.

Incorporation of basic nitrogen-containing functional groups onto the LDPE substrates was accomplished by allylamine ( $\text{CH}_2=\text{CHCH}_2\text{NH}_2$ ) plasma polymerization. However, unavoidable large amounts of oxygen-containing functionalities were also incorporated when using this system. Large amounts of these oxygen species were incorporated by post-plasma-treatment reaction with atmospheric oxygen.

ESCA results showed that the largest amount of nitrogen-containing functional group incorporation resulted from the 5 W plasma excitation energy. Ten watt plasma energies were the least effective in the incorporation of nitrogen-containing functional groups for the allylamine plasmas. Surface concen-

trations of nitrogen-containing functionalities decreased with time due to the diffusion of these hydrophilic functional groups into the bulk of the materials with time. ESCA results also showed that surface oxygen concentrations of the allylamine plasma polymers increased with time. Air and *n*-octane in water contact-angle measurements revealed an increase of surface hydrophilicity with time because of the large extent of post-plasma-treatment surface oxidation. ATR-FTIR spectroscopy was able to qualitatively identify a number of nitrogen- and oxygen-containing functional groups in the allylamine plasma polymer.

The allylamine plasma polymers showed poor thromboresistance. There were more platelets and higher percentages of spreading and fully spread platelets adhering to the plasma-treated materials than to the base LDPE. The difference of plasma energy levels in the preparation of test samples had a minimal effect on thrombogenicity.

Profilometry results indicated that the plasma polymer deposition rate of acrylic acid was about seven times that of allylamine under similar monomer gas flow conditions. In the plasma polymerization of allylamine, surface roughness increased as the plasma excitation energy increased. In contrast,

the surfaces of acrylic acid plasma polymers were smooth and the surface morphologies were independent of the plasma energy used.

This work was supported by the NSF Plasma-Aided Manufacturing Engineering Research Center at the University of Wisconsin-Madison under Grant No. CDR-8721545. Mr. Jui-Che Lin and Dr. John R. Jacobs provided invaluable technical assistance during the construction of the plasma reactor system. Dr. Steven L. Goodman provided assistance with the experimental procedures for the platelet adhesion studies. Mr. Quintin J. Lai helped with the analysis of the SEM micrographs.

## REFERENCES

1. H. Yasuda, *Plasma Polymerization*, Academic Press, Orlando, FL, 1985.
2. W. R. Gombotz and A. S. Hoffman, *CRC Crit. Rev. Biocompat.*, **4**(1), 1 (1987).
3. A. S. Hoffman, *J. Appl. Polym. Sci. Appl. Polym. Symp.*, **42**, 251 (1988).
4. Y. S. Yeh, Y. Iriyama, Y. Matsuzawa, S. R. Hanson, and H. Yasuda, *J. Biomed. Mater. Res.*, **22**, 795 (1988).
5. H. Biederman and Y. Osada, *Adv. Polym. Sci.*, **95**, 57-109 (1990).
6. H. Hettlich, F. Otterbach, Ch. Mittermayer, R. Kaufmann, and D. Klee, *Biomaterials*, **12**, 521 (1991).
7. S. I. Ertel, B. D. Ratner, and T. A. Horbett, *J. Biomed. Mater. Res.*, **24**, 1637 (1990).
8. M. Karakelle, N. Shields, D. D. Solomon, and R. A. Taller, in *Society for Biomaterials 15th Annual Meeting Abstracts*, 1989, p. 238.
9. J. R. Hollahan and T. Wydeven, *Science*, **179**, 500 (1973).
10. J. Sakata, M. Yamamoto, and M. Hirai, *J. Appl. Polym. Sci.*, **37**, 2773 (1989).
11. C. N. B. Tran and D. R. Walt, *J. Colloid Interface Sci.*, **132**, 373 (1989).
12. W. R. Gombotz and A. S. Hoffman, *J. Appl. Polym. Sci. Appl. Polym. Symp.*, **42**, 285 (1988).
13. F. Tanfani, A. A. Durrani, M. Kojima, and D. Chapman, *Biomaterials*, **11**, 585 (1990).
14. K. Allmér, J. Hilborn, P. H. Larsson, A. Hult, and B. Rånby, *J. Polym. Sci. A Polym. Chem.*, **28**, 173 (1990).
15. H. Iwata, A. Kishida, M. Suzuki, Y. Hata, and Y. Ikada, *J. Polym. Sci. A Polym. Chem.*, **26**, 3309 (1988).
16. B. D. Ratner, *Ann. Biomed. Eng.*, **11**, 313 (1983).
17. *The Standard Infrared Prism Spectra*, Sadtler Research Laboratories, Philadelphia, PA, 1963.
18. S. R. Holmes-Farley, C. D. Bain, and G. M. Whitesides, *Langmuir*, **4**, 921 (1988).
19. A. R. Thompson and L. A. Harker, *Manual of Hemostasis and Thrombosis*, 3rd ed., F. A. Davis Co., Philadelphia, 1983.
20. M. D. Lelah and S. L. Cooper, *Polyurethanes in Medicine*, CRC, Boca Raton, FL, 1986.
21. C. Fougnot, D. Labarre, J. Jozefonvicz, and M. Josefowicz, in *Macromolecular Biomaterials*, G. W. Hastings and P. Ducheyne, Eds., CRC, Boca Raton, FL, 1984.
22. P. N. Walsh and J. H. Griffin, *Blood*, **57**, 106 (1981).
23. S. L. Goodman, private communication.
24. T.-M. Ko, PhD Thesis, University of Wisconsin-Madison, 1991.
25. T. Yasuda, T. Okuno, K. Yoshida, and H. Yasuda, *J. Polym. Sci. B Polym. Phys.*, **26**, 1781 (1988).
26. M. Morra, E. Occhiello, and F. Garbassi, *Adv. Colloid Interface Sci.*, **32**, 79 (1990).
27. Y. Iriyama, T. Yasuda, D. L. Cho, and H. Yasuda, *J. Appl. Polym. Sci.*, **39**, 249 (1990).
28. S. L. Goodman, Masters Thesis, University of Wisconsin-Madison, 1984.
29. J. A. Chinn, B. D. Ratner, and T. A. Horbett, to appear.

Received October 2, 1991

Accepted January 13, 1992